



PERGAMON

International Journal of Impact Engineering 23 (1999) 981–988

www.elsevier.com/locate/ijimpeng

INTERNATIONAL
JOURNAL OF
IMPACT
ENGINEERING

APPLIED RESEARCH OF SHAPED CHARGE TECHNOLOGY

YU CHUAN, TONG YANJIN, YAN CHENGLI, LI FABO, GUI YULIN,
ZHANG MING, WANG BINGREN, XIE PANHAI, and LI LIANGZONG

(Laboratory for Shock Wave and Detonation Research ,
Institute of Fluid Physics, CAEP, P.O.Box 523, Chengdu ,610003,CHINA)

Summary—For special requirements of penetrating rock, we have developed a shaped charge jet device, from which a rather uniform and wide jet can be generated. The mass of shaped charge explosive is less than 2.5kg. The profile and velocity of the jet are measured with an X-ray technique. We have simulated the formation and penetration process of the jet with a 2-D HELP code, which provides important reference data in designing the shaped charge. A series of penetration tests into rock at different strengths has been carried out. The penetration tests to the rock with a strength about 600kg/cm² show that the average diameter of the hole entrances is 63.5 mm; the average penetration depth of the holes with internal diameters of more than 35 mm is about 1311 mm, the average total penetration depth of the holes is 1531 mm; the coning of the holes are less than 1.4 %. All the results of the tests indicate good penetrating performance.

Additionally, we have designed an explosively formed projectile (EFP) testing device with the explosive of 450g, a liner of 150g and 60mm-diameter. Performance tests and experiments of penetrating multilayer steel plates have been conducted. The EFP penetrates throughout the whole steel target that consists of five layers of 6-mm-thick A3 steel plate spaced in a range of two meters. The diameters of penetrating holes range from 41mm to 46mm. The mass of EFP recovered behind the target is about 98g. © 1999 Elsevier Science Ltd. All rights reserved.

INTRODUCTION

Since World War II, shaped charge technology has been rapidly developed. Generally, the shaped charge has two forms : jet and explosively formed projectile (EFP).

Research in jet technology has been mainly focused on the design of armor penetration warhead for several decades^[1,2] As the increasing needs from military engineering and civilian uses, the technology of penetration to non-metal targets (e.g., concrete, rock, etc.) has been widely investigated. For example, jet technology has been used for rapid construction of military protection engineering. Shaped charge warheads have been designed for use against the piers, blockhouses, and strong aboveground fortifications. Additionally, the shaped charge technology has been used to penetrate holes in petroleum prospecting. In 1983, M.J. Murphy, who worked with the Lawrence Livermore National Laboratory (LLNL), investigated jet penetration in concrete^[3]

For EFP, applications include semi-armor piercing warheads for anti-ship missiles. Through a design of several liners for the semi-armor piercing warhead, the warhead will explode within the ship to form several EFPs that penetrate multi-separators. This will significantly increase the destroying capability of a warhead. It is now a major trend to apply the EFP technology to warheads of advanced anti-ship missiles. For example, the EFP technology is used in German

Kormoran II anti-ship missile warheads.

JET PENETRATION TO ROCK

The jet must be wider and more uniform to obtain deep penetration depth and a large penetration diameter to meet the requirement of a second explosion within the hole. The slug must be as small as possible to increase the mass of the jet. Additionally, it is essential that the jet have a moderate velocity and velocity gradient so as not to make the jet break out while reaching the target surface.

With an optimum design of the shaped charge and the liner with a curved surface and varying thickness, we have designed the jet devices with two different liners through a numerical simulation with a 2-D HELP code and experimental adjustments. The shaped charge explosive has a density of 1.80g/cm^3 is HMX/TNT (70/30).

Two jet devices was considered. The first one has a liner made up of pure copper. The diameter of the liner is 140mm; the mass of the liner is 1.0kg; the mass of explosive is 2.3kg; and the total mass of this device is about 3.8kg. Figure 1 gives a schematic diagram of the jet device. The second one has a liner made up of aluminum. The diameter of the liner is 141mm, and the mass about 0.62kg; the mass of explosive about 2.5kg; and the total mass of the device is about 3.7kg.

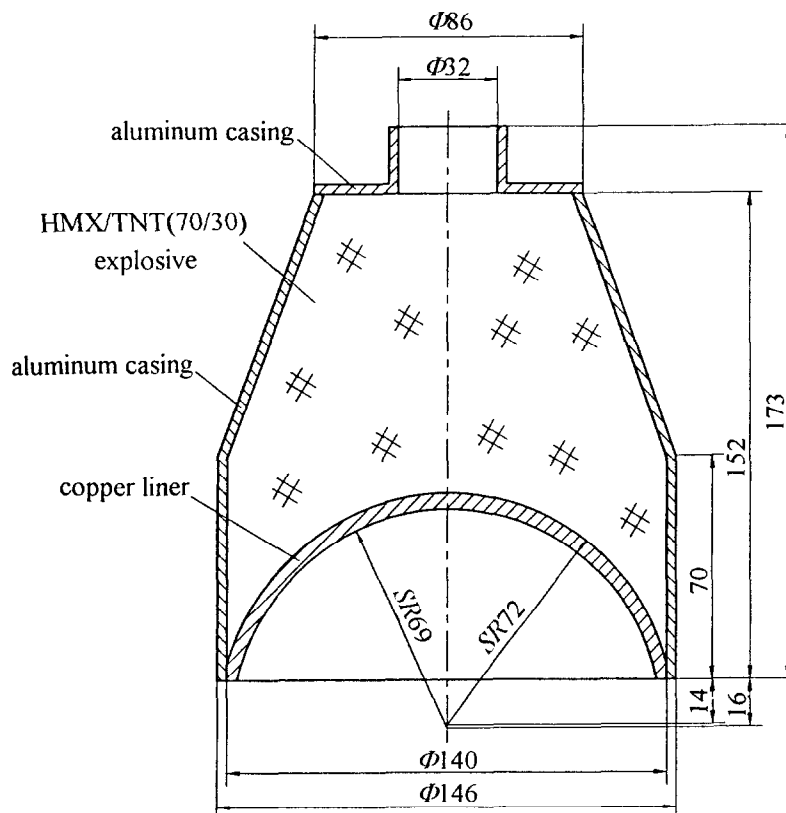


Fig. 1. A schematic diagram of the jet device

Measurement with X-rays

We measured, with X-ray photography, the profile and velocity of the jet generated by the copper liner device (see figure 2).

We can find from Fig.2 that the jet was wide and uniform. Velocity of the head part of the jet is 3.63km/s. At about 261.19 μ s after the primer detonation, the jet has almost reached the target surface. There is not any fracture except for a small piece in the head part of the jet. The slug is very small. Not considering the slug and the broken piece in the head part of the jet, the length of the jet is 581mm. The diameters of the head and tail parts of the jet are 6.9mm and 21.4mm, respectively.

Rock Penetration Experiments

For the above two jet devices, we have conducted penetration experiments to rocks of different strengths. The industrial primer-8 and a tetryl booster charge (32mm diameter, 11mm length) were used to initiate the charge in these experiments. The experimental setup is shown in Fig.3.

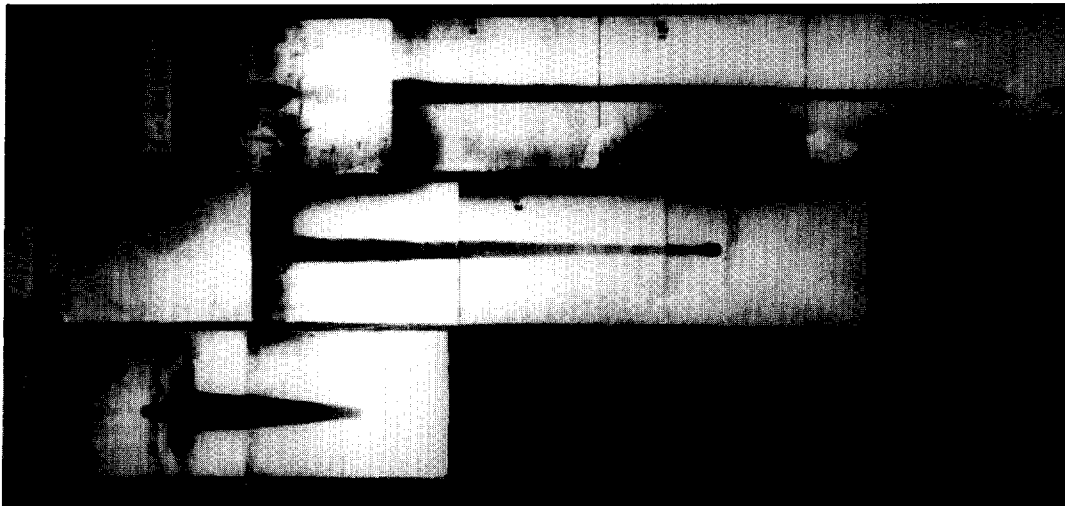


Fig.2. An X-ray photograph of the jet generated by the copper liner device

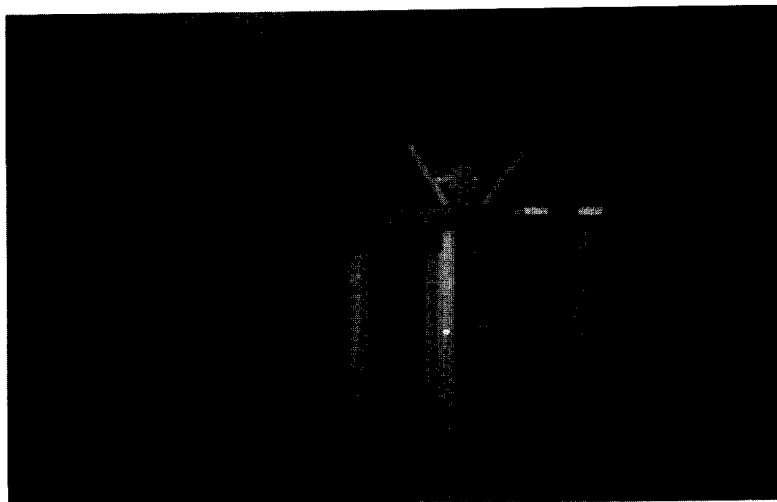


Fig.3. An experimental setup of rock penetration

With copper liner charge, we have carried out eight penetration experiments to three kinds of rocks of different strengths. The typical penetration result is shown in Fig. 4 and a sketch of the penetration channel profile is depicted in Fig.5, from which we can find that there is pit with funnel forms. There is a circular and straight deep hole at the bottom of the pit. The hole is uniform internally with no cracks, dilapidation or blockage.

In order to measure the hole's coning, we use a cylindrical stick that has diameters (d_2) of 30mm, 35mm, and 40mm respectively to measure the depth (L_2) of diameter larger than d_2 . The hole's coning can be described as the following,

$$k = \frac{d_3 - d_2}{2(L_2 - L_1)} \tag{1}$$

where, d_3 is the diameter of the hole entrance; L_1 is the total depth of the pit. The test results are listed in Table 1.



Fig.4. A result of penetration to the rock surface

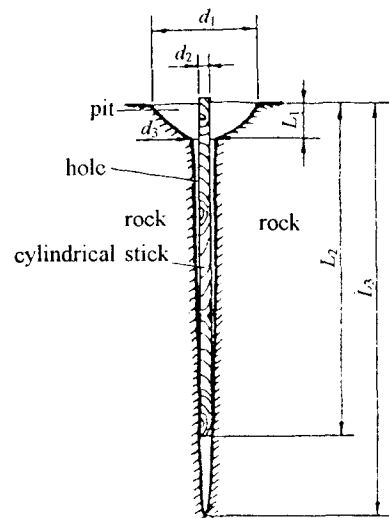


Fig.5. A sketch map of measurement of penetration effects

Table 1. Penetration test results from the copper liner device

No.	σ /(kg/cm^2)	H /mm	D_1 /mm	d_3 /mm	L_1 /mm	L_2 /mm			L_3 /mm	V / cm^3	k /($\%$)
						$d_2=30\text{mm}$	$d_2=35\text{mm}$	$d_2=40\text{mm}$			
1	1400	1000	300	43	105	530	—	—	605	4782	1.5
2	1400	1100	370	45	145	605	—	—	625	9906	1.6
3	1400	1100	400	40	110	700	—	—	750	8121	0.9
4	1000	1000	260	45	70	515	—	—	1425	2963	1.7
5	600	1080	400	52	135	1510	1230	—	1630	11264	0.8
6	600	1030	420	61	120	1270	1240	—	1275	11227	1.2
7	600	950	250	69	80	1450	1250	—	1540	4835	1.4
8	600	1025	250	72	90	1525	1525	1200	1680	5770	1.3

In Table 1, σ represents the strength of the rock; H is the stand off; d_1 is the diameter of the pit entrance; L_3 is the total penetration depth; and V is the penetration volume.

From Table 1, we can find that, for the three penetration tests to the hard rock with a strength of 1400 kg/cm^2 , the average diameter of the hole entrance is 43mm; the average penetration depth for the holes with diameters of more than 30mm is about 612mm; the average penetration depth is 660mm; the average penetration volume is 7603 cm^3 ; and the average coning is about 1.33%. For the hard rock with a strength of 1000 kg/cm^2 , these values are respectively 45mm, 515mm, 1425mm, 2963 cm^3 , and 1.7%.

We have also carried out four tests for the rock with a strength of 600 kg/cm^2 . Of these tests, the smallest diameter of the hole entrance is 52mm and the average is 63.5mm. The average penetration depth for the hole with diameters of more than 35mm is about 1311mm. The smallest penetration depth is 1275mm, and the average one for the four tests is 1531mm. The average penetration volume of these tests is 8274 cm^3 . The biggest hole coning of the tests is 1.4%, and the average coning is about 1.2%.

Additionally, for the aluminum liner charge device, we have conducted three penetration tests to the rock with two different strengths. The test results are listed in Table 2.

Table 2. Penetration test results from the aluminum liner device

No.	σ /(kg/cm^2)	H /mm	d_1 /mm	d_3 /mm	L_1 /mm	L_2/mm			L_3 /mm	V / cm^3	k /(%)
						$d_2=30\text{mm}$	$d_2=35\text{mm}$	$d_2=40\text{mm}$			
1	1400	945	900	75	200	430	420	—	430	68310	9.1
2	1400	1200	530	55	140	555	—	—	650	17499	3.0
3	1000	1200	530	68	75	—	1400	875	1500	10999	1.2

From Table 2, for the hard rock with a strength of 1400 kg/cm^2 , the average diameter of the hole entrance of the two tests is 65mm. The average penetration depth for the holes with diameters of larger than 30mm is about 493mm. The average penetration depth is 540mm; the penetration volume of 42905 cm^3 ; and the hole coning about 6.1%. For the hard rock with strength of 1000 kg/cm^2 , the diameter of the hole entrance is 68mm. The penetration depths are respectively 1400mm and 875mm for the hole with diameters of larger than 35mm and 40mm. The total penetration depth is 1500mm, the volume of 10999 cm^3 , and the hole coning about 1.2%.

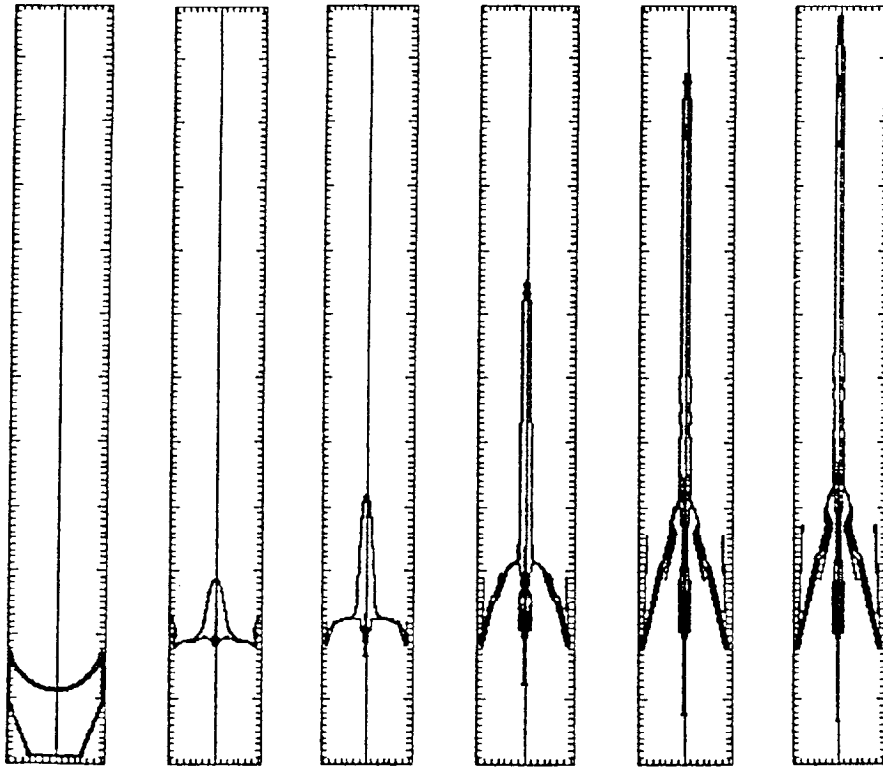
Numerical Simulation

The jet formation and penetrating process in the rock are numerically simulated with a 2-D Eulerian elastic-plastic hydrodynamic code (HELP). The jets are respectively generated by a pure copper liner charge and an aluminum liner charge^[4]. The simulation results of the pure copper liner charge are given in Figure 6 and 7.

From Fig.6, we can find that the results from numerical simulations agree very well with those from X-ray measurements shown in Fig.2. The jet velocity determined from numerical simulation is about 3.87 km/s. At the time of $261 \mu\text{s}$, the jet length is 866.5mm that is a little more than that from X-ray measurement. The largest penetration depth obtained by numerical simulation is 1560mm; and the average diameter of the hole is about 35mm. Both agree with the experimental results.

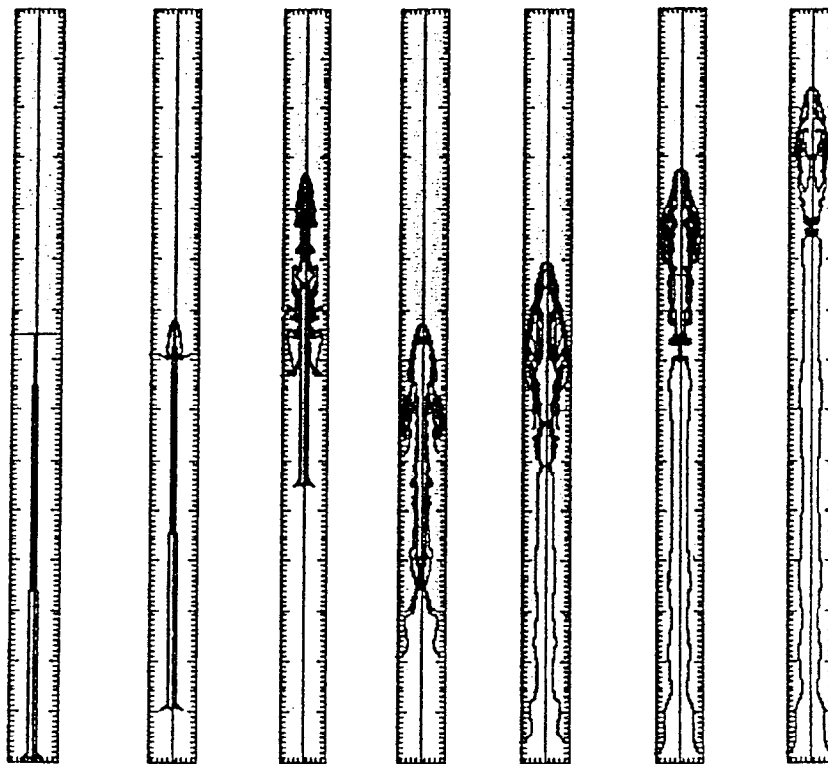
EFP PENETRATING A TARGET OF MULTILAYER STEEL PLATES

We have designed a small EFP testing device. TNT/RDX (40/60) explosive with density of 1.70 g/cm^3 is used. The mass of the explosive is 450g. The mass of the liner is 150g and its diameter is 60mm. The setup of the testing device is given in Fig.8. The profile and velocity of the EFP are measured by X-rays photography and shown in Fig.9.



(a) $t=0\mu\text{s}$; (b) $t=60\mu\text{s}$; (c) $t=91\mu\text{s}$; (d) $t=175\mu\text{s}$; (e) $t=261\mu\text{s}$; (f) $t=281\mu\text{s}$

Fig. 6. Numerical simulation of the jet formation generated by the pure copper liner charge



(a) $t=0\mu\text{s}$; (b) $t=50\mu\text{s}$; (c) $t=272\mu\text{s}$; (d) $t=472\mu\text{s}$; (e) $t=692\mu\text{s}$; (f) $t=900\mu\text{s}$; (g) $t=1100\mu\text{s}$

Fig. 7. Numerical simulation of the jet penetrating process in the rock for pure copper liner charge

We can find from Fig.9 that the EFP has an ideal profile. The ratio of length-to-diameter is 1.32 and the largest diameter is about 32mm. The mass of the EFP is 127g and velocity of 1.52km/s.

Three tests of penetration to a target consisting of multilayer steel plates have been carried out. The plate array consisted of 6-mm-thick A3 steel plate; five plates were used, uniformly spaced over a range of two meters. The EFP testing device is two meters from the first layer of the target. The EFPs penetrate all target elements; the diameters of the penetrating holes range from 41mm to 46mm. A photograph of the hole on the fifth layer of steel plate in the third test is given in Fig.10.

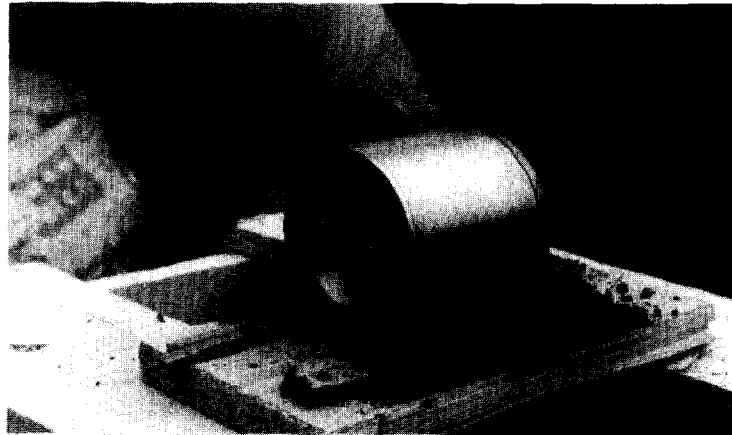


Fig.8. A photograph of EFP testing device

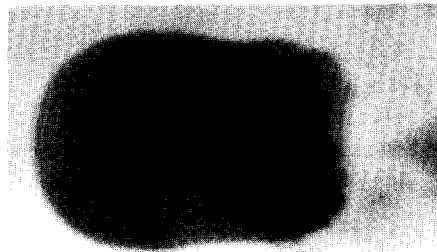


Fig.9. An EFP Profile measured by X-rays



Fig.10. A hole on the fifth layer of steel plate

After penetrating throughout multilayers of steel plate, the EFP does not break into pieces on the whole. An intact EFP of 98g is recovered behind the target.

CONCLUSIONS

1) In designing the liner of the jet device, a technique of curved surface and varying thickness was used. With precise calculations and experiment adjustment, the mass of the jet converted from the liner is increased. The jet is thus uniform and wide that is suitable for penetrating rock. The jet also has a proper velocity distribution.

2) In designing the charge of the jet device, a coning structure of the charge is used, which increases the utilization coefficient of the energy of explosive and decreases the mass of the shaped charge, thus the total mass of the jet device.

3) We have done some work on the fundamental principles of the jet penetration to the rock. Performance of the jet generated from different metal materials and the penetration effects to the rock with different strengths are also investigated. We have fundamentally known well the design of shaped charge that can meet the requirements of both the penetration diameter and depth.

4) The jet and EFP devices we have designed have good penetration effects.

Acknowledgement — The authors thank the following colleagues for their help to the work. They are Zhang Kejian, Sun Chengwei, Liu Guangzou, Jiang Hongzi, Liu Daming, Ding Baoxian, Zang Zentao, Li Yu, Gu Xingrong, Ren Huiqi, Yang Renhua, Mi Zongchueng, Gao Zhenghong, et al.

REFERENCES

- 1 Kivity Y, Maysel M, et al. An Efficient Model for Shaped Charge Design. 7th Symp.(Int.) on Ballistics, 1983.
- 2 Xie Panhai, Su Linxiang, et al. Ring Initiation for Improving Shaped Charge Performance. 13th Symp.(Int.) on Ballistics, Sweden, 1992.
- 3 Murphy M J. Shaped Charge Penetration in Concrete: A Unified Approach. UCRL-53393, 1983.
- 4 Hagaman L J. HELP: A Multi-Material Eulerian Program for Compressible Fluid and Elastic-Plastic Flows in Two Space Dimensions and Time. AD-726459, AD-726460, 1971.